

# Synthesis, Crystal Structures, and Electronic Properties of Nonlinear Fused Thienoacene Semiconductors

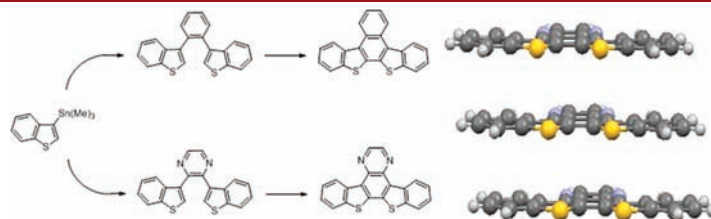
Hayden T. Black, Shubin Liu,<sup>†</sup> and Valerie Sheares Ashby\*

Department of Chemistry, University of North Carolina, Chapel Hill, North Carolina 27599, United States, and Research Computing Center, University of North Carolina, Chapel Hill, North Carolina 27516, United States

ashby@email.unc.edu

Received October 16, 2011

## ABSTRACT

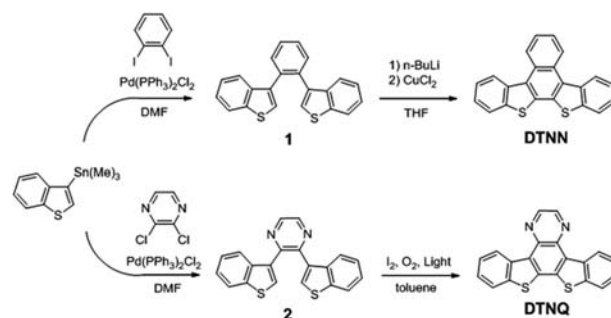


Two fused thienoacene compounds with two-dimensional ring connectivity were synthesized, and their semiconducting properties were characterized. Both compounds have a crystal structure comprised of herringbone arrays of tight  $\pi$ - $\pi$  stacks. Strong  $\pi$ - $\pi$  interactions lead to self-assembly into well-defined crystalline thin films from the vapor phase for both compounds. Field effect transistors were fabricated, affording identical hole mobilities of  $3.0 \times 10^{-3} \text{ cm}^2/(\text{V s})$  and  $I_{\text{on/off}} > 10^5$ .

Fused polycyclic aromatic compounds are at the forefront of organic semiconductor (OSC) research due to their high charge mobilities. Some of the highest hole mobilities for OSCs have been discovered using single crystals of fused acenes such as pentacene<sup>1</sup> and rubrene.<sup>2</sup> Efficient charge transport within these materials is attributed to their planar structures and extended  $\pi$ -conjugation which leads to good  $\pi$ - $\pi$  overlap in the solid state. Thienoacene compounds have also emerged as high performance semiconductors due to their high charge mobilities and improved stabilities compared to acenes.<sup>3–7</sup> The aromatic ring connectivity has been shown to greatly affect the HOMO orbital geometries and crystal structures

for thienoacene compounds,<sup>8</sup> properties that dictate charge mobility. Therefore, significant research has been directed toward understanding structure property relationships within thienoacene materials.

## Scheme 1. Synthesis of DTNN and DTNQ



In this work we report the synthesis and characterization of naphtho[2,1-*b*:3,4-*b'*]bis[1]benzothiophene (DTNN) and quinoxalo[6,5-*b*:7,8-*b'*]bis[1]benzothiophene (DTNQ),

(8) Takimiya, K.; Shinamura, S.; Osaka, I.; Miyazaki, E. *Adv. Mater.* **2011**, *23*, 4347.

<sup>†</sup> Research Computing Center.

(1) Jurchescu, O. D.; Baas, J.; Palstra, T. T. M. *Appl. Phys. Lett.* **2004**, *84*, 3061.

(2) Hasegawa, T.; Takeya, J. *Sci. Technol. Adv. Mater.* **2009**, *10*, 024314.

(3) Takimiya, K.; Ebata, H.; Sakamoto, K.; Izawa, T.; Otsubo, T.; Kunugi, Y. *J. Am. Chem. Soc.* **2009**, *128*, 12604.

(4) Ebata, H.; Izawa, T.; Miyazaki, E.; Takimiya, K.; Ikeda, M.; Kuwabara, H.; Yui, T. *J. Am. Chem. Soc.* **2007**, *129*, 15732.

(5) Yamamoto, T.; Takimiya, K. *J. Am. Chem. Soc.* **2007**, *129*, 2224.

(6) Shinamura, S.; Osaka, I.; Miyazaki, E.; Nakao, A.; Yamagishi, M.; Takeya, J.; Takimiya, K. *J. Am. Chem. Soc.* **2011**, *133*, 5024.

(7) Zschieschang, U.; Ante, F.; Yamamoto, T.; Takimiya, K.; Kuwabara, H.; Ikeda, M.; Sekitani, T.; Someya, T.; Kern, K.; Klauk, H. *Adv. Mater.* **2010**, *22*, 982.

two nonlinear fused thienoacenes with a unique ring connectivity (Scheme 1). DTNN was previously synthesized using a different route via Nagao et al. but was not studied as a semiconductor.<sup>9</sup> Compound DTNN is isoelectronic with the two-dimensional hydrocarbon benzo[*s*]picene, a material which has also not yet been explored for semiconductor applications.<sup>10</sup> Two-dimensional (2-D) aromatic connectivity has been shown to lead to high charge mobilities in thienoacene semiconductors<sup>11</sup> and may promote strong  $\pi$ - $\pi$  interactions in the solid state. Compound DTNQ incorporates a pyrazine ring to study the effects of nitrogen incorporation on the thienoacene system. Pyrazine rings have previously been shown to effectively modulate HOMO and LUMO energies in fused acenes,<sup>12,13</sup> but nitrogen incorporation has not yet been explored within thienoacene structures.

A similar synthetic route was used to construct both molecules, although different reactions were utilized in the aromatic cyclization (Scheme 1). Photocyclooxidation was ideal for compound DTNQ since the reaction only requires solvent and catalytic iodine and leads to a pure crude product free of metals. Attempts to photocyclize compound **1** resulted in poor conversion; therefore, DTNN was synthesized using the copper promoted coupling of dilithiated **1**.

Both compounds are wide band gap semiconductors with optical band gaps of 3.33 eV for DTNN and 2.97 eV for DTNQ. DTNN is a white solid whereas DTNQ is yellow. Both compounds show two maxima in the near-UV

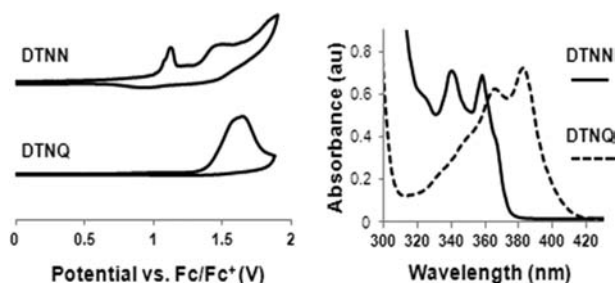


**Figure 1.** Oxidative cyclic voltammograms (left) and UV/vis spectra in THF solutions (right).

resulting from vibronic coupling of the  $\pi$ - $\pi^*$  transition (Figure 1). This behavior is common for rigid thienoacenes

(9) Nagao, I.; Shimizu, M.; Hiyama, T. *Angew. Chem., Int. Ed.* **2009**, *48*, 7573.

(10) Tang, X.-Q.; Harvey, R. G. *J. Org. Chem.* **1995**, *60*, 3568.

(11) Brusso, J. L.; Hirst, O. D.; Dadvand, A.; Ganesan, S.; Cicoira, F.; Robertson, C. M.; Oakley, R. T.; Rosei, F.; Perepichka, D. F. *Chem. Mater.* **2008**, *20*, 2484.

(12) Gao, B.; Wang, M.; Cheng, Y.; Wang, L.; Jing, X.; Wang, F. *J. Am. Chem. Soc.* **2008**, *130*, 8297.

(13) Richards, G. J.; Hill, J. P.; Subbaiyan, N. K.; D'Souza, F.; Karr, P. A.; Elsegood, M. R. J.; Teat, S. J.; Mori, T.; Ariga, K. *J. Org. Chem.* **2009**, *74*, 8914.

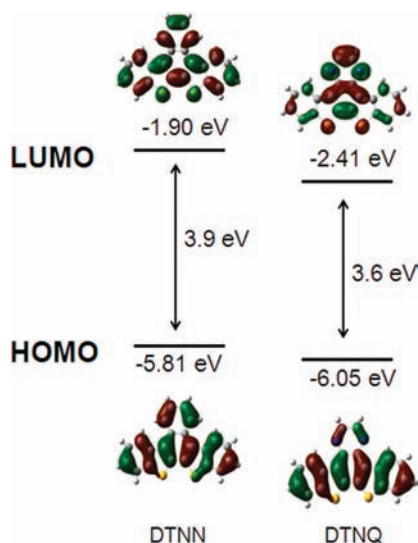
(14) Sánchez-Carrera, R. S.; Delgado, M. C. R.; Ferrón, C. C.; Osuna, R. M.; Hernández, V.; Navarrete, J. T. L.; Aspuru-Gazik, A. *Org. Electron.* **2010**, *11*, 1701.

which have limited conformational disorder as a result of their fused structures.<sup>14</sup> The quinoxaline ring in DTNQ leads to a relatively large reduction of the band gap due to the donor-acceptor-like structure.

Electrochemically determined HOMO levels are  $-5.93$  eV for DTNN and  $-6.26$  eV for DTNQ (Figure 1), whereas DFT calculations predict  $-5.81$  eV for DTNN and  $-6.05$  eV for DTNQ. Compared to other thienoacene compounds, the calculated and electrochemically determined HOMO levels of DTNN are exceptionally low.<sup>8</sup> This is a result of the 2-D aromatic ring connectivity, which results in diminished aromaticity and a lower lying HOMO.<sup>8,15</sup> HOMO orbital surfaces show large extended lobes on the thiophene rings for both compounds (Figure 2). Contribution from sulfur to the HOMO is small compared to other thienoacenes. The electron distribution is spread evenly in two dimensions for DTNN, whereas DTNQ has a HOMO that is more localized on the lower five rings.

LUMO levels calculated from the electrochemical HOMO plus the optical band gap are  $-2.60$  eV for DTNN and  $-3.29$  eV for DTNQ. Thus, incorporation of the nitrogen-rich ring leads to a much larger reduction in LUMO (0.69 eV) than HOMO (0.33 eV). This finding suggests that increasing the nitrogen content in structurally similar compounds could lead to very low LUMO levels and may be a useful strategy for the design of n-type semiconductors.

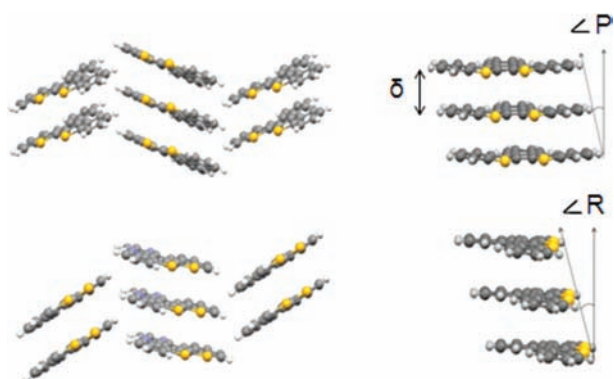
Crystal structure analysis is an important tool for considering charge transport in organic semiconductors, since charge mobility is dependent on electronic communication between nearest neighbors in the solid state. Some efforts have been directed toward crystal engineering of face-to-face  $\pi$ -stacks,<sup>16</sup> a departure from the often observed herringbone motif in many OSCs. However,



**Figure 2.** Calculated frontier orbitals of DTNN and DTNQ (density functional theory, B3LYP/6-311+G\* level).

**Table 1.** Crystallographic Data for DTNN and DTNQ

	DTNN	DTNQ
space group	$C_2/c$	$P_{21/n}$
$a$ (Å)	38.108	20.351
$b$ (Å)	3.838	3.788
$c$ (Å)	21.281	21.243
$\beta$ (deg)	108.880	118.588
$\tau$ (deg)	70.59	77.90
$\delta$ (Å)	3.488	3.479
pitch (deg)	15.81	6.87
Roll (deg)	20.31	21.69

**Figure 3.** Herringbone packing motif for DTNN (left, top) and DTNQ (left, bottom) and illustration of pitch and roll angles (right).

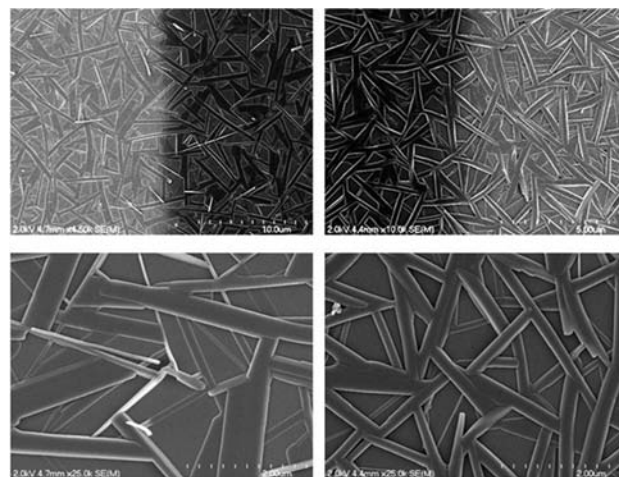
some evidence suggests that the herringbone structure is advantageous for 2-D charge transport and can lead to higher mobilities than simple  $\pi$ -stacked structures.<sup>8</sup>

Single crystals as large as 3 mm were easily obtainable for both compounds during purification steps. Crystals of DTNN were obtained via recrystallization from toluene whereas DTNQ crystals were grown through sublimation. Both compounds exhibit a layered structure comprised of tight  $\pi$ -stacks aligned along the  $b$ -axis, arranged into herringbone arrays (Figure 3). DTNN has a slight molecular curvature with a maximum torsion angle of 3.9°, while DTNQ is completely planar. Compared to other thienoacenes, DTNN and DTNQ have large  $\tau$  values, the angle between the molecular plane and the stacking axis (Table 1). This, combined with the small pitch and roll angles for both compounds, leads to a large  $\pi$ -overlap within the stacking direction. The molecular stacking distance along the  $b$ -axis is only  $\sim 3.48$  Å for both compounds, further demonstrating the strong intermolecular interactions within these solids.

(15) Suresh, C. H.; Gadre, S. R. *J. Org. Chem.* **1999**, *64*, 2505.

(16) Chang, Y.-C.; Chen, Y.-D.; Wen, Y.-S.; Lin, J.-T.; Chen, H.-Y.; Kuo, M.-Y.; Chao, I. *J. Org. Chem.* **2008**, *73*, 4608.

Unlike most other thienoacenes, DTNN and DTNQ have both S-atoms on the same side of the ring, leading to isolated sulfur interactions in the crystal structure. Thus, sulfur is not expected to play a large role in charge transport for these materials. In fact, DTNN does not have any sulfur contacts less than the sum of the van der Waals radii. In contrast DTNQ has a short S–S (3.553 Å) contact and also possesses a short S–C contact (3.494 Å) within the  $\pi$ -stacking direction. The pitch angle for DTNQ is less than half of that for DTNN, increasing

**Figure 4.** SEM images of DTNN (left) and DTNQ (right). Lighter regions in top images are the gold source/drain electrodes.

the amount of  $\pi$ – $\pi$  interactions in the stacking direction. In addition, N-atoms in DTNQ show H-bonding, leading to tighter packing and a slight increase in the density of the solid ( $\rho = 1.536$  mg/mm<sup>3</sup> for DTNN,  $\rho = 1.582$  mg/mm<sup>3</sup> for DTNQ). Thus, nitrogen incorporation leads to increased intermolecular interactions in the solid state.

Scanning electron microscopy (SEM) was used to study the morphologies that arise from vapor deposition of the two compounds. Films were grown via sublimation onto an octyltrichlorosilane treated Si/SiO<sub>x</sub> wafer (Figure 4). Film thicknesses were 80–100 nm, consisting of well-defined crystals 2–8  $\mu$ m in length. The high aspect ratio of the crystals clearly demonstrates preferred growth parallel to the plane of the substrate. This is consistent with growth along the  $b$ -axis, which is considerably shorter than that along the other axes of the unit cell for both compounds. The distinct crystallites shown in Figure 4 are not typical structures for thienoacene thin films, which more often form continuous films comprised of terrace-like grains.<sup>5,17,18</sup> The 1-D self-assembly of DTNN and DTNQ could be useful for the construction of discrete semiconducting components (i.e., molecular wires).

(17) Laquindanum, J. G.; Katz, H. E.; Lovinger, A. J. *J. Am. Chem. Soc.* **1998**, *120*, 664.

(18) Izawa, T.; Miyazaki, E.; Takimiya, K. *Adv. Mater.* **2008**, *20*, 3388.

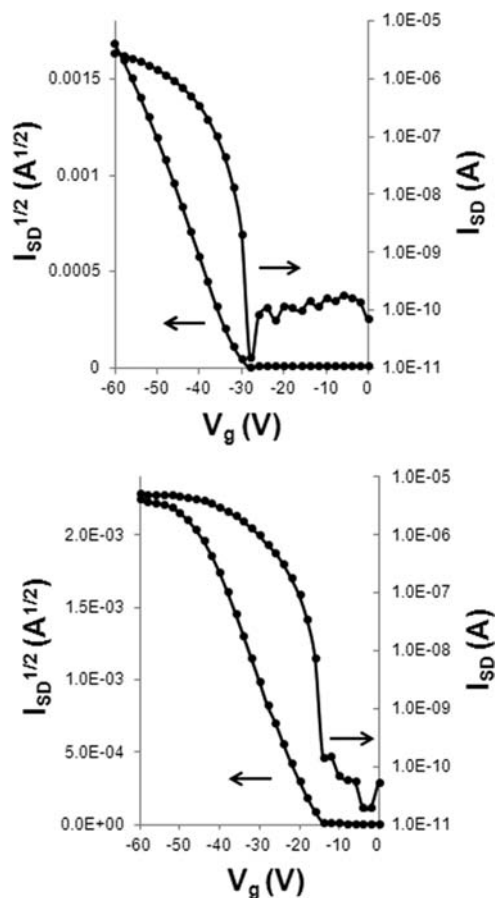


**Figure 5.** Transfer characteristics of DTNN (top) and DTNQ (bottom) transistors.

Formation of such well-defined crystallites is mainly attributed to highly preferred growth along the short  $b$ -axis, which is comprised of strong  $\pi$ -stacks. Similar behavior was reported for a sickle shaped thienoacene that possessed a similarly short  $a$ -axis (3.883 Å), as well as a similar molecular stacking distance (3.53 Å).<sup>19</sup>

Top contact-bottom gate FET devices were fabricated to study the charge mobility of DTNN and DTNQ. P-type field effect behavior was observed for both compounds (Figure 5). Output characteristics show deviation from linearity at low  $V_{SD}$  for both compounds (SI Figure 1), indicating some contact resistance. This is likely due to significant charge injection barriers as a result of the large

(19) Li, R.; Dong, H.; Zhan, X.; He, Y.; Li, H.; Hu, W. *J. Mater. Chem.* **2010**, *20*, 6014.

difference between the work function of gold and the HOMO levels of the semiconductors.

Average hole mobilities for the two compounds were found to be identical at  $3.0 \times 10^{-3} \text{ cm}^2/(\text{V s})$ . Charge transport is therefore very similar within these two materials, a direct result of their similar HOMO orbital geometries, crystal structures, and thin film morphologies. These hole mobilities are relatively modest compared to other thienoacenes.<sup>8</sup> However, we note that the obtained thin film morphologies are not ideal for charge transport and likely restrict mobility due to limited surface coverage and large angle grain boundaries. On/off currents for devices were  $10^5$ – $10^6$  while threshold voltages were not stable, shifting to larger values from scan to scan. The low HOMO levels of DTNN and DTNQ are expected to result in very stable materials; therefore the instability of  $V_T$  is likely due to adsorption of  $\text{H}_2\text{O}/\text{O}_2$  on the exposed dielectric.

In conclusion, we have synthesized two new thienoacene semiconductors with 2-D ring connectivity. The compounds crystallize into the common herringbone motif and exhibit exceptional  $\pi$ – $\pi$  overlap. Strong  $\pi$ – $\pi$  interactions in the solid leads to self-assembly into well-defined 1-D microcrystals upon sublimation. Similar FET properties were observed for both compounds with hole mobilities of  $3.0 \times 10^{-3} \text{ cm}^2/(\text{V s})$  and  $I_{\text{on/off}}$  of  $10^5$ – $10^6$ . We expect that improvements in charge mobilities for these compounds will be possible through further optimization of the thin film morphology and device geometry.

**Acknowledgment.** We thank Amar Kumbhar at the Chapel Hill Analytical and Nanofabrication Laboratories (CHANL) for help with SEM images. We also thank Dr. Peter White, director of the X-ray Facility at the University of North Carolina at Chapel Hill, for technical assistance with crystal structure determination. A portion of this work was performed in the UNC EFRC Instrumentation Facility funded by the UNC EFRC: Solar Fuels and Next Generation Photovoltaics, an Energy Frontier Research Center funded by the U.S. Department of Energy, Office of Science, Office of Basic Energy Sciences under Award Number DE-SC0001011 and by UNC SERC: “Solar Energy Research Center Instrumentation Facility” funded by the U.S. Department of Energy, Office of Energy Efficiency & Renewable Energy under Award Number DE-EE0003188

**Supporting Information Available.** Synthesis, characterization, crystallographic files, and device fabrication. This material is available free of charge via the Internet at <http://pubs.acs.org>.